

In Situ Gel-to-Crystal Transition and Synthesis of Metal Nanoparticles Obtained by Fluorination of a Cyclic β -Aminoalcohol Gelator

Yang Xu,^[a, b] Chuanqing Kang,^{*[a]} Yu Chen,^[a] Zheng Bian,^[a] Xuepeng Qiu,^[a] Lianxun Gao,^{*[a]} and Qingxin Meng^[b]

Abstract: A new fluorinated version of a cyclic β -aminoalcohol gelator derived from 1,2,3,4-tetrahydroisoquinoline is presented. The gelator is able to gel various nonprotic solvents through OH \cdots N hydrogen bonds and additional CH \cdots F interactions due to the introduction of fluorine. A bimolecular lamellar structure is formed in the gel phase, which partly preserves the pattern of molecular organization in the single crystal. The racemate of the chiral gelator shows lower gelation ability than its enantiomer because of a higher tendency to form microcrystals, as shown by X-ray diffraction analysis. The influence of fluorination on the self-assembly of the gelator and the properties of

the gel was investigated in comparison to the original fluorine-free gel system. The introduction of fluorine brings two new features. The first is good recognition of *o*-xylene by the gelator, which induces an in situ transition from gels of *o*-xylene and of an *o*-xylene/toluene mixture to identical single crystals with unique tubular architecture. The second is the enhanced stability of the toluene gel towards ions, including quaternary ammonium salts, which enables the preparation of a stable toluene gel

in the presence of chloroaurate or chloroplatinate. The gel system can be used as a template for the synthesis of spherical gold nanoparticles with a diameter of 5 to 9 nm and wormlike platinum nanostructures with a diameter of 2 to 3 nm and a length of 5 to 12 nm. This is the first example of a synthesis of platinum nanoparticles in an organogel medium. Therefore, the appropriate introduction of a fluorine atom and corresponding nonbonding interactions into a known gelator to tune the properties and functions of a gel is a simple and effective tactic for design of a gel system with specific targets.

Keywords: fluorine • gels • gel-to-crystal transition • nanoparticles • self-assembly

Introduction

Low-molecular-mass organogelators (LMOGs) have attracted much attention from the chemistry community owing to their applications in various interdisciplinary fields.^[1] Driven by multiple weak nonbonding interactions,^[2] the LMOGs self-aggregate into entangled 3D nanofibrous networks that immobilize liquids through surface tension and capillary forces.^[3] Control and exploitation of supramolecular gelation are important aspects of the grand challenge of directed assembly of extended structures with targeted properties.^[4] One facile tactic to tune the properties or functions of a gel

is to integrate an original gelator structure with new groups that can provide new driving forces or specific functions. A small structural change could have a great influence on the self-assembly of a gelator and the organization of 3D nanofibrous networks, which subsequently changes the macroscopic properties.^[5] Understanding certain fundamental aspects, such as the self-assembly mechanisms of LMOGs, control of molecular packing in the fibers of a gel, and the relationship between the molecular packing in gelation and crystallization, are primary requirements for effective manipulation of the gel formation and for designing new LMOGs.^[6] A few examples of in situ gel to single crystal transitions have opened up investigation of the organization and mechanisms of molecule aggregates in gel state,^[7,8] which are also interesting topics from a physical viewpoint.^[9]

In particular, few fluorinated LMOGs with unique properties and functions, such as the gelation of perfluorocarbons or supercritical carbon dioxide and templating of fluorinated silica nanomaterials, have been reported.^[10] R. G. Weiss et al. described the design of fluorine-containing three-component gelators to tune molecular aggregation and gel stability.^[11] K. L. Caran et al. made a comparison between the gelation properties of fluorinated and nonfluorinated propargylic alcohols, in which weak CH \cdots F interactions were proposed to play a role in the self-assembly of the gelators.^[12]

[a] Y. Xu, Dr. C. Kang, Y. Chen, Dr. Z. Bian, Prof. Dr. X. Qiu, Prof. Dr. L. Gao
State Key Laboratory of Polymer Physics and Chemistry
Changchun Institute of Applied Chemistry
Chinese Academy of Sciences
5625 Renmin Street, Changchun 130022 (China)
Fax: (+86) 431-85262926
E-mail: kangcq@ciac.jl.cn
lxgao@ciac.jl.cn

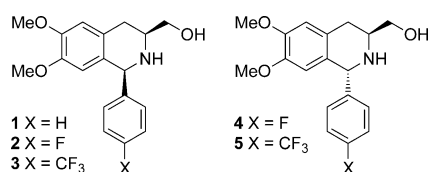
[b] Y. Xu, Dr. Q. Meng
Department of Polymer Materials
Changchun University of Technology
2055 Yan'an Street, Changchun 130022 (China)

Supporting information for this article is available on the WWW under <http://dx.doi.org/10.1002/chem.201202615>.

Fluorine seems to be an indispensable structural factor for gelation in these cases. The strongly electronegative fluorine atom usually forms strong interactions with electrophilic atoms, such as the CH...F bonding observed in crystallography.^[13] However, no report has ever clarified the generic role of fluorine in the formation of gel phase.

An exciting application of gels is as a template in the synthesis of metal nanoparticles.^[14] There have been a number of reports on the growth of metal nanoparticles, such as silver nanoparticles and gold nanoparticles (AuNPs), within the gel matrix.^[15] A. K. Das reported the only example to date of the synthesis of platinum nanoparticles (PtNPs) in bolaamphiphile hydrogels.^[16] The formation and size of nanoparticles within the gel phase are controlled by tunable cages that effectively separate metal ions to prevent the aggregation of metal particles on reduction.^[17] The challenge is to form the desired small particles with narrow size distribution. The common requirements for gels to template the synthesis of metal nanoparticles are sufficient stability towards metal ions, compatibility with surfactants and stabilizers, and stabilization of the nanoparticles. We are also interested in the synthesis of metal nanoparticles with a gel system that fulfills these requirements.

With this knowledge in hand, we investigated whether and how fluorine provides nonbonding intermolecular interactions to determine the self-aggregation of molecules into organogels. A cyclic β -aminoalcohol organogelator (**1**) based on the 1,2,3,4-tetrahydroisoquinoline (THIQ) scaffold (Scheme 1) was synthesized and characterized in our previous study.^[18] Herein, we incorporate fluorine into the cyclic β -aminoalcohol to evaluate the influence of a fluorine atom on the self-assembly and gelation properties. Molecules **2–5**, in which fluorine or trifluoromethyl replace the corresponding proton on **1**, are considered (Scheme 1). We present the results of the influence of the fluorination on gelation, in situ phase transition, and stability towards ions. The enhanced stability enables the synthesis of metal nanoparticles by using this gel system.



Scheme 1. THIQ-based cyclic β -aminoalcohols

Results and Discussion

Synthesis: Enantiomeric aminoalcohols **2–5** were prepared from L-DOPA by using known procedures;^[18,19] the racemate of **2** was synthesized by methods we previously reported.^[20] All structures were confirmed by using 1D and 2D NMR spectroscopy and mass spectroscopy (the synthesis and characterizations are given in detail in the Supporting Information).

Gel test: The gelation ability of molecules **2–5** in various common solvents was tested by using the inverted-tube method. Compounds **3–5** showed good solubility but no gelation ability in all tested solvents. Compound **2** formed an organogel in most of the tested solvents, as summarized in Table 1. The minimum gelation concentration (MGC) of **2** is 0.8, 0.5, 0.6, 0.9, 2.5, and 4.0 % g mL^{-1} in benzene, toluene, *o*-xylene, chlorobenzene, acetonitrile, and ethyl acetate at 20 °C, respectively. Chloroform, dichloromethane, and tetrahydrofuran could be gelled by **2** below 0 °C at a concentration of 5.0 % g mL^{-1} , but the gels quickly convert to solutions at room temperature.

Table 1. Gelation by **2** and its racemate.^[a]

| Solvent | 2 | <i>rac-2</i> |
|------------------|-------------------------|-------------------|
| benzene | CG (0.8) | CG (2.0) |
| toluene | CG (0.5) | CG (0.9) |
| <i>o</i> -xylene | CG (0.6) | CG (2.4) |
| chlorobenzene | CG (0.9) | CG (2.0) |
| acetonitrile | CG (2.5) | OG (4.8) |
| ethyl acetate | CG (4.0) | PG ^[c] |
| chloroform | CG (5.0) ^[b] | – ^[d] |
| dichloromethane | CG (5.0) ^[b] | – ^[d] |
| tetrahydrofuran | CG (5.0) ^[b] | – ^[d] |

[a] Gelation was measured with inverted-tube method at 20 °C; only solvents gelled by **2** are listed; CG = clear gel, OG = opaque gel, PG = partial gel; numbers in parenthesis are minimum gelation concentrations [% g mL^{-1}]. [b] Gels were formed below 0 °C. [c] Concentration > 5.0%. [d] Not measured.

The range of solvents gelled by **2** is narrower than that of its nonfluorinated analogue **1**, given that alcohols and ketones cannot be gelled by **2**. The reason for this may be the high potential of protic solvents (alcohols) or solvents with active α -protons (ketones) to form hydrogen bonds with fluorine atoms, which would interrupt the gelator–gelator interactions responsible for gelation.^[21] The poor gelation ability of **4** compared with its epimer **2** suggests the importance of the *cis* arrangement of 3-hydroxymethyl to 1-aryl for gelation. Molecules **3** and **5**, which contain a trifluoromethyl group, may afford better compatibility with solvent molecules to give better solvation of the gelators. Gelation arises from a balance between solvent–gelator interactions and gelator–gelator interactions. Therefore, good solvation would damage aggregation of gelators and result in the poor gelation ability of molecules **3–5**, which is very similar to the empirical understanding of gelation manipulated by different peripheral groups or solvents.^[21]

Molecule *rac-2* displays gelation ability with higher MGC values of 2.0, 0.9, 2.4, 2.0, and 4.8 % g mL^{-1} in benzene, toluene, *o*-xylene, chlorobenzene, and acetonitrile, respectively. A partial gel is formed in ethyl acetate at 5 % g mL^{-1} . The gelation ability of *rac-2* is not as good as its enantiomer **2**.

Micromorphology: Micromorphological investigations of the xerogels of **2** were carried out by using scanning electronic microscopy (SEM) techniques. The images in Figure 1 show the subtle influence of the solvent on the formation of the

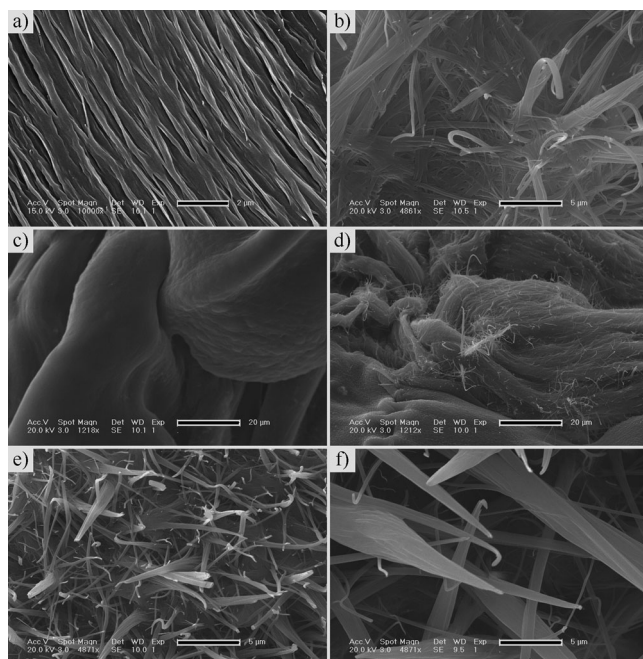


Figure 1. SEM images of xerogels from a) toluene, b) *o*-xylene, c) benzene, d) chlorobenzene, e) ethyl acetate, and f) acetonitrile. Scale bars: 2 (a), 5 (b, e, f), and 20 μm (c, d).

fibrous networks. Well-developed fibrous networks that range in size from the nano- to micrometer scale are formed in all solvents except benzene, in which a crinkled film is formed. This film may be derived from the entanglement of thin fibrous networks. The xerogel of the chlorobenzene gel is composed of recognizable fibers that are woven into a compact network like the film in benzene. Polar solvents, such as ethyl acetate and acetonitrile, seem to favor the formation of rigid nanofibers. SEM images of xerogels from toluene and *o*-xylene display a remarkable difference in that toluene induces bundles of nanofibers in a parallel arrangement whereas *o*-xylene produces distinctive nanofiber micromorphology. The gel fibers in *o*-xylene extend randomly, which indicates that the solvent separates the nanofibers more effectively than toluene. The fiber–fiber interactions in *o*-xylene are disrupted to a similar degree as in polar solvents, which implies subtle difference in the properties of the toluene and *o*-xylene gels.

Gel-to-crystal transitions and single crystal analysis: Most of the gels of **2** are stable enough to survive long-term standing. However, an exception is the *o*-xylene gel, which is spontaneously converted into a single crystal on standing for around 2 d at room temperature. As shown in Figure 2, a few crystals appear in the gel matrix, followed by collapse of the gel into a solution with more crystal particles. The gelator tends to be precipitated directly from *o*-xylene if the concentration is greater than 3% g mL^{-1} . The in situ transition from organogel to single crystals affords an opportunity for deep insights into the self-assembly of the gelator.

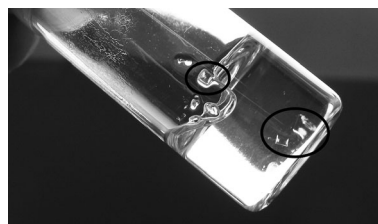


Figure 2. Crystals formed by an in situ gel-to-crystal transition in *o*-xylene gel.

The crystals of **2** from *o*-xylene gel are suitable for X-ray single-crystal analysis, and display a monoclinic system with $P2_1$ space group. As shown in Figure 3a, each unit cell is composed of two gelator molecules and two *o*-xylene molecules. The molecules of **2** are arranged parallel to the *ac* plane through $\text{OH}\cdots\text{N}$ hydrogen bonds (1.906 \AA) to form a linear aggregate along the *b* axis, in which two adjacent molecules are assembled in a staggered head-to-head manner (Figure 3b). Additional $\text{CH}\cdots\text{F}$ interactions (2.552 \AA) between the fluorine atoms in one linear aggregate and the methoxy protons in another linear aggregate drive the formation of a tubular architecture along the *b* axis, with a diameter of about 8 \AA , which acts as a host for *o*-xylene mole-

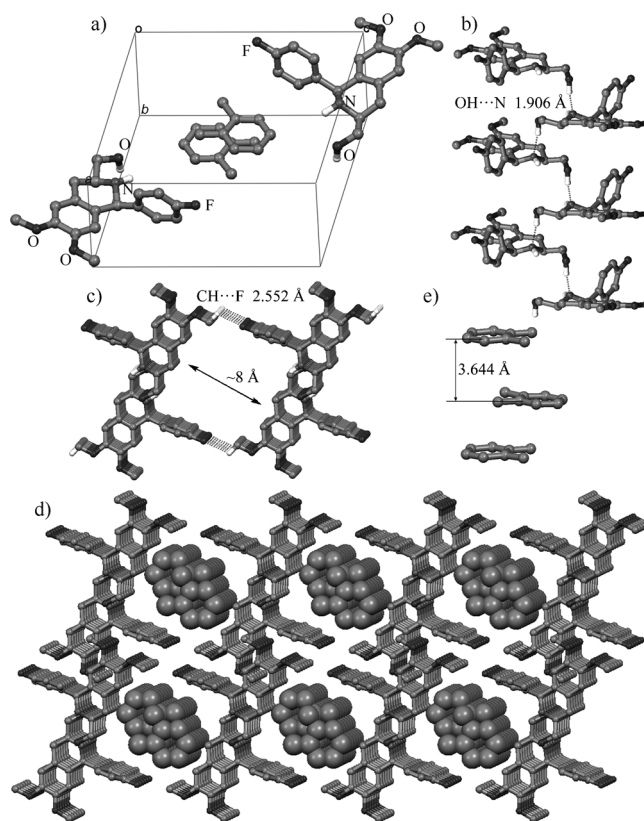


Figure 3. Single-crystal analysis of **2**, showing a) the unit cell; b) the linear aggregation of the gelator through $\text{OH}\cdots\text{N}$ hydrogen bonds; c) the cyclic tetramer formed by $\text{OH}\cdots\text{N}$ and $\text{CH}\cdots\text{F}$ interactions; d) multi-tubular stacking forms host sites for *o*-xylene molecules; e) parallel stacking of *o*-xylene along the *b* axis. For clarity, only hydrogen atoms on heteroatoms or involved in nonbonding interactions in a), b), and c) are shown.

cules (Figure 3c). The tubular structure extends along the *a* and *c* axes to form a multitubular aggregate through van der Waals and CH \cdots F interactions, respectively (Figure 3d). The solvent molecules are encapsulated in the multitubular structures and constrained in antiparallel stacks by weak CH \cdots π interactions between the methyl and aryl moieties of adjoining *o*-xylene molecules (Figure 3e).

Further experiments were carried out to understand the role of toluene and *o*-xylene in the self-assembly of the gelators. A gel of a *o*-xylene/toluene mixture (1:1) can convert into a single crystal with exclusive inclusion of *o*-xylene in the same stacking pattern as that of crystals from the *o*-xylene gel. A single crystal with same architecture was also obtained on concentration of a dilute solution of **2** in a mixture of *o*-xylene and toluene (1:1) under a weak nitrogen flow. The ratio of solvents was changed to about 95:5 when the crystals had formed. This solvent selectivity suggests high recognition of the spatial size and shape of *o*-xylene molecules during assembly of the gelators.^[22] A toluene gel collapses and converted to crystals if it is covered with *o*-xylene for two weeks. It is likely that dissolution of fibrous network of the toluene gel and crystal formation take place in combination with diffusion of *o*-xylene into the gel phase.

The gel phase is an important transition state for the self-assembly of the fluorinated gelator. The gel-to-crystal transition is considered to be a stage in the route from gelation through dissociation to crystallization.^[8,23] In the case of the fluorinated gel system, competition between the two phases favors crystallization in the presence of *o*-xylene, which helps break the metastable gelation structure and promote stable crystal aggregation. It is likely that *o*-xylene repairs defects in the molecular self-assembly in the gel phase and stabilizes the tubular structure of the gelators in the crystal phase. The in situ transition from gel to single crystal reveals an evolution of the self-assembly of the fluorinated gelators from low orderliness to high orderliness, in which both additional CH \cdots F interactions and the appropriate spatial size and architectural adjustment of solvent molecules are important factors.

Powder XRD analysis of xerogel 2: As shown in Figure 4a, the simulated XRD pattern of a single crystal of **2** demonstrates a significant diffraction at (001) with a *d*-spacing of 13.26 Å that corresponds to the space of the tubular structure along the *c* axis. The diffraction at (100) with a *d*-spacing of 12.16 Å corresponds to the hydrogen-bond-driven staggered head-to-head arrangement, the space of the tubular structure along the *a* axis.

Elucidation of the aggregation of molecules in the gel fibers was carried out by using powder XRD analysis for xerogel **2** from toluene. Attempts to prepare xerogel from *o*-xylene failed to crystallize during solvent evaporation. As shown in Figure 4b, the broad peaks at *d*-spacings of 18.1, 8.7, 6.2, and 4.5 Å correspond to a lamellar structure. The diffractions are attributable to the (100) plane given the hierarchical self-assembly of the gelators and the high similarity between the XRD patterns of xerogel **2** and xerogel **1**.^[18]

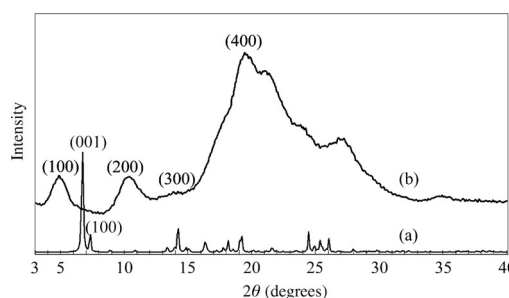


Figure 4. a) The simulated XRD of a single crystal of **2** from *o*-xylene and b) the powder XRD of xerogel **2** from toluene.

The strongest intermolecular interactions in the gel system are the hydrogen bonds between hydroxy and amine groups, which spontaneously initiate the self-assembly of free molecules into head-to-head bimolecular units and subsequently to linear aggregates. The lateral fluorine atoms drive the side-by-side arrangement of the linear aggregates through CH \cdots F interactions that extend to form a bimolecular layer with a space of around 18.1 Å, equivalent to the (100) plane of the single crystal (Figure S1 in the Supporting Information). The packing pattern of molecules in the single crystal is partially preserved in the gel phase.

A few studies have reported differences in gelation ability between the enantiomer and the racemate of an organogelator;^[24] in one of our studies we revealed the reason for this difference at the molecular level.^[7] For this fluorinated β -aminoalcohol gelator, the gelation ability of *rac*-**2** is lower than its enantiomeric counterpart. The powder XRD pattern of xerogel *rac*-**2** from toluene (Figure 5) provides clues for this difference. The diffractions at *d*-spacings of 17.2, 8.6, 5.8, 4.4, and 3.4 Å are attributed to a lamellar structure in the xerogel. However, all the diffractions are far sharper and narrower than those of the enantiomer. In addition, there are also a few other sharp diffractions that do not appear in the XRD pattern of the enantiomer. These results strongly suggest that the molecules are aggregated in a more regular and orderly arrangement. It is likely that the gel of *rac*-**2** is comprised of a lot of microcrystals that are responsible for the higher orderliness.

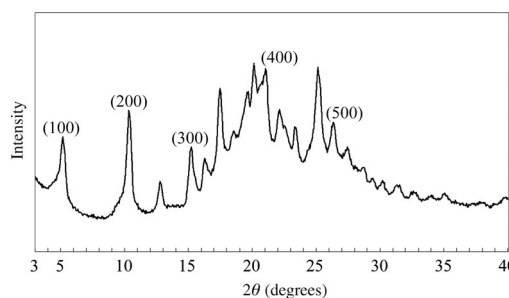


Figure 5. The powder XRD pattern of xerogel of *rac*-**2** from toluene.

Stability towards ions: The stability of the toluene gel towards ions was evaluated by contact with an aqueous solution of metal ions, and the durability of fluorinated gelator **2**

was compared with that of nonfluorinated gelator **1**.^[18] The experiments were carried out by covering a toluene gel with aqueous solutions of metal ions. The gels of fluorinated gelator **2** displayed enhanced stability. The toluene gel of **2** remains stable in the presence of many metal ions, such as Li^+ , Na^+ , K^+ , Mg^{2+} , Ca^{2+} , Zn^{2+} , Mn^{2+} , Co^{2+} , and Ni^{2+} ions, which is in agreement with the results for the toluene gel of **1**. In the presence of Fe^{3+} and Cu^{2+} ions, it takes 4 to 5 d for the toluene gel of **2** to be completely destroyed. In contrast, the collapse of the toluene gel of **1** takes less than 10 h. In the presence of Ag^+ ions, the gel of **2** is completely destroyed within 30 min, which is far faster than the nonfluorinated gel system. The reason for this is the strong interactions between Ag^+ and the fluorine groups. Significantly, the toluene gel of **2** is stable in the presence of quaternary ammoniums, such as tetraoctylammonium bromide (TOAB), chloroaurate (TOA-Au), or chloroplatinate (TOA-Pt), whereas the toluene gel of **1** is quickly converted into loose gel blocks that disperse into clear solvent. The enhanced stability sheds light on the effects of the introduction of fluorine and related interactions that tune the gel system to stronger stability towards specific ions.

Synthesis of gold and platinum nanoparticles: The synthesis of small AuNPs and PtNPs was carried out on the merits of the stability of the toluene gel of **2** towards TOA-Au and TOA-Pt. The metal nanoparticles were prepared by mixing an aqueous solution of hydrogen chloroaurate or hydrogen chloroplatinate (0.06 M, 0.8 mL) with toluene (5.4 mL) that contained TOAB (0.048 and 0.12 mmol for chloroaurate and chloroplatinate, respectively). The biphasic mixture was stirred vigorously before the color of aqueous layer turned colorless. The higher concentration of TOAB in toluene for chloroplatinate ions guarantees uniformity and stability of the TOA-Pt in toluene. The red organic layer was separated to give a TOA-Au or TOA-Pt solution with a concentration of 0.009 M, and stored at ambient temperature in the absence of light. Gelator **2** (30 mg) was dissolved in the toluene solution of TOA-Au or TOA-Pt (1.0 mL) by heating. A gel containing TOA-Au or TOA-Pt was formed on cooling and standing at room temperature. The toluene solution of TOA-Au and the gelator turned from red to colorless before gelation, which indicated reduction of Au^{3+} to Au^+ by the gelators.^[25] The TOA-Pt-containing solution did not show this phenomenon. Both metal ions in gels can be reduced to zero valency by being covered with aqueous sodium borohydride (0.2 M, 0.8 mL).^[16,26,27] The AuNPs-containing gel changed color to dark purple whereas the PtNPs-containing gel is off-white.

The gold and platinum nanoparticles in the xerogels were observed by using transmission electron microscopy (TEM). The TEM images of the AuNPs-containing xerogel indicate the presence of spherical nanoparticles with diameters of 5 to 9 nm (Figure 6a and b). The fact that the AuNPs are clearly arranged along the gel nanofibers suggests effective separation of gold ions (Au^{3+} and Au^+) by the aggregates of the gelators. The low-valence gold ions (Au^+) may have

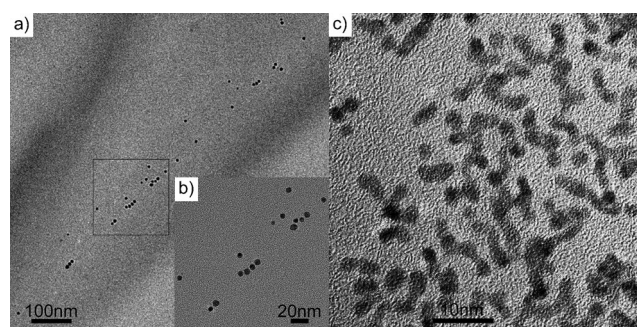


Figure 6. TEM images of a) AuNPs in xerogel matrix; b) enlargement of the region highlighted by a rectangle in a); and c) PtNPs in the xerogel matrix.

coupled with the gelators on reduction from Au^{3+} . The aggregation of AuNPs is also inhibited by their absorbance on the surface of the nanofibers.^[28] The compositions of the AuNPs was confirmed by using energy-dispersive X-ray analysis (EDX, Figure S2 in the Supporting Information).

The TEM images of PtNPs-containing xerogels display a different micromorphology and dispersion. A small amount of spherical nanoparticles and a large amount of wormlike nanostructures are observed and are scattered across the field of view (Figure 6c). The diameter of the spherical nanoparticles and wormlike nanostructures is 2 to 3 nm and the length of the wormlike structures ranges from 5 to 12 nm. The wormlike PtNPs predominate over the spherical structures. The composition of the PtNPs was confirmed by using EDX (Figure S3 in the Supporting Information). Extensive scattering of the PtNPs that is not limited to the gel fibers suggests poor interactions between the chloroplatinate ions and the gel fibers or gelators. The chloroplatinate ions are probably shielded by excess TOABs. Tetraalkylammonium salts were used as a soft template for the synthesis of metal nanoparticles by mediating shape and dispersion of metal ions.^[27,29] In this fluorinated gel system, the chloroplatinate ions are considered to be encapsulated within the surfactant tetraoctylammonium. The gel serves as a supporting system to cage the TOA-Au and control the distribution and shape within a stable fibrous network. The PtNPs should be scattered in the spaces between the gel fibers.

The gel system of **2** can be used as a template and container for AuNPs and PtNPs due their stability towards TOA-Au and TOA-Pt and consequently their ability to stabilize the nanoparticles. This advancement relies on the introduction of fluorine into the original cyclic β -aminoalcohol, **1**. The properties of the metallic ions and the use of the surfactant result in different distributions and shapes of AuNPs and PtNPs.

Conclusion

In summary, we have developed a new fluorinated version of a cyclic β -aminoalcohol gelator and evaluated the influence of the introduced fluorine on the gel properties and ap-

plications. Fluorinated cyclic β -aminoalcohol **2** and its racemate are able to gel several common nonprotic solvents. A single crystal obtained from the *o*-xylene gel of **2** by an in situ gel-to-crystal transition shows a tubular structure composed of gelators taking part in unique OH \cdots N hydrogen bonds and CH \cdots F interactions and filled with *o*-xylene molecules. Single crystals grown from the gel of a mixture of toluene and *o*-xylene have identical crystal architecture, which indicates high selectivity for and recognition of *o*-xylene during the self-assembly of the gelators. A lamellar structure with bimolecular layers is formed in the gel phase of **2** and *rac*-**2** according to the XRD patterns, and was compared to the structure of the single crystal. The introduction of a fluorine and subsequently additional CH \cdots F interactions enhances the stability of the toluene gel towards ions, including TOA-Au and TOA-Pt. AuNPs and PtNPs were prepared by using the toluene gel as a template. Spherical AuNPs with a diameter of 5 to 9 nm were arranged along the gel fibers, whereas wormlike PtNPs with a diameter of 2 to 3 nm and a length of 5 to 12 nm predominated in number over spherical PtNPs with a diameter of 2 to 3 nm. This is the first synthesis of PtNPs by using an organogel.^[16] Therefore, the introduction of fluorine atoms and CH \cdots F interactions significantly change the properties of the gel system and offer applications in nanoparticles synthesis. These results demonstrate simple and effective tactics to tune the properties and functions of gelators, which we believe to be useful for the design of gel system. Further studies of applications of the gold and platinum nanocomposites in catalysis are in progress.

Experimental Section

Materials and methods: All reagents and solvents were commercially available and used without further purification. Molecules **2–5** were synthesized according to literature procedures and are detailed in the Supporting Information. SEM images were recorded by using an XL 30 ESEM FEG field emission scanning electron microscope. Powder XRD patterns were recorded by using a Rigaku D/max 2000 X-ray diffractometer equipped with a Cu $_{K\alpha 1}$ radiation source. X-ray single crystallographic analysis was performed by using a Bruker SMART APEX II CCD diffractometer with graphite-monochromatic Mo $_{K\alpha}$ radiation ($\lambda = 0.71073$ Å). The crystal structures were solved by direct methods using the SHELXL-97 program and refined with anisotropic thermal parameters by full matrix least squares on F^2 values with SHELXL-97.^[30] TEM images were recorded by using a TECNAI G2 high-resolution transmission electron microscope operated at an acceleration voltage of 200 kV. EDX was carried out to confirm the nanoparticles compositions by using an EDAX detector coupled with TEM. Samples were prepared by wiping a carbon-coated copper grid on nanoparticles-contained gel followed by natural evaporation of the solvent.

Gel preparation: An accurately weighed amount of gelator (2–3 mg) was added to a glass vial that contained solvent (1 mL) and sealed. The suspension was then heated to give a homogeneous solution that was then left to cool to RT. After 30 min at RT, if no gel was formed, more gelator (1–2 mg) was added and dissolved in the solution by heating. The procedure was repeated until a gel formed, at which point the concentration of gelator in the solvent was recorded to give the MGC value. For racemic gelator *rac*-**2**, several hours of standing at RT was sometimes required to form a gel.

Crystallization of 2: The single crystals for X-ray crystallography analysis were prepared by three methods. The first two methods were in situ transitions from gels: a gel of **2** prepared in *o*-xylene (0.8% g mL $^{-1}$) or from a mixture of toluene and *o*-xylene (1:1, 1% g mL $^{-1}$) was allowed to stand at RT and single crystals formed in the gel within 2 or 3 d. The third method involved formation from a solution: a solution of **2** in a mixture of toluene and *o*-xylene (1:1, 0.5% g mL $^{-1}$) was placed under a weak nitrogen flow, and the *o*-xylene/toluene ratio increased to more than 95:5, as determined by gas chromatography, as the single crystal formed. The structural information and crystal data are listed in Table 2. CCDC-874186 (**2**) contains the supplementary crystallographic data for this paper. These data can be obtained free of charge from The Cambridge Crystallographic Data Centre via www.ccdc.cam.ac.uk/data_request/cif.

Gel stability towards ions: Gel stability towards cations was tested by covering a toluene gel of **2** (1 mL, 0.8% g mL $^{-1}$) with a fresh solution of cation (0.1 mmol metal ion in 1 mL deionized water). The bilayer sample (aqueous upper layer) was left to stand for at least one week to determine the time for gels to be completely broken down.

Synthesis of gold nanoparticles: Hydrogen tetrachloroaurate(III) trihydrate (18.6 mg, 0.047 mmol) was dissolved in deionized water (0.8 mL).

Table 2. Single-crystal data for **2** formed from *o*-xylene gel (method 1), xylene/toluene gel (method 2), and xylene/toluene solution (method 3).

| | Method 1 | Method 2 | Method 3 |
|---------------------------------------|--|--|--|
| formula | C ₁₈ H ₂₀ FNO ₃ ·C ₈ H ₁₀ | C ₁₈ H ₂₀ FNO ₃ ·C ₈ H ₁₀ | C ₁₈ H ₂₀ FNO ₃ ·C ₈ H ₁₀ |
| M_r | 423.51 | 423.51 | 423.51 |
| crystal system | monoclinic | monoclinic | monoclinic |
| space group | $P2_1$ | $P2_1$ | $P2_1$ |
| a [Å] | 12.403(2) | 12.324(2) | 12.341(2) |
| b [Å] | 7.2868(13) | 7.1557(13) | 7.1652(11) |
| c [Å] | 13.523(2) | 13.305(2) | 13.369(2) |
| α [°] | 90.00 | 90.00 | 90.00 |
| β [°] | 101.350 | 99.788 | 99.926(3) |
| γ [°] | 90.00° | 90.00 | 90.00 |
| V [Å ³] | 1198.3(4) | 1156.2(4) | 1164.5(3) |
| Z | 2 | 2 | 2 |
| ρ_{calcd} [g cm $^{-3}$] | 1.174 | 1.216 | 1.208 |
| μ [mm $^{-1}$] | 0.081 | 0.084 | 0.084 |
| T [K] | 293(2) | 293(2) | 295(2) |
| crystal form | block | block | block |
| crystal size [mm] | 0.32 × 0.21 × 0.10 | 0.21 × 0.15 × 0.10 | 0.31 × 0.22 × 0.11 |
| crystal color | colorless | colorless | colorless |
| absorption correction | multi-scan | multi-scan | multi-scan |
| total data collected | 7161 | 5677 | 6338 |
| unique data observed | 4192 | 2830 | 3368 |
| data | 3429 | 1995 | 2833 |
| $[I > 2\sigma(I)]$ | | | |
| R_{int} | 0.0162 | 0.0443 | 0.0303 |
| θ_{max} [°] | 25.02 | 25.02 | 26.00 |
| index range | $-12 \leq h \leq 14$ $-8 \leq k \leq 8$ $-16 \leq l \leq 14$ | $-14 \leq h \leq 14$ $-8 \leq k \leq 5$ $-15 \leq l \leq 15$ | $-15 \leq h \leq 15$ $-4 \leq k \leq 8$ $-16 \leq l \leq 16$ |
| R_1 | 0.0580 | 0.1118 | 0.0590 |
| $[I > 2\sigma(I)]$ | | | |
| $wR(F^2)$ | 0.1693 | 0.2738 | 0.1524 |
| $[I > 2\sigma(I)]$ | | | |
| R_1 , all data | 0.0698 | 0.1376 | 0.0693 |
| $wR_2(F^2)$, all data | 0.01875 | 0.3031 | 0.1634 |
| S | 0.924 | 1.143 | 1.013 |
| parameters | 272 | 284 | 284 |

The aqueous solution was then added to a solution of TOAB (48.0 mg, 0.149 mmol) in toluene (5.4 mL) and stirred vigorously until all the red color had transferred from the aqueous layer into the organic layer. The organic layer was separated by using a pipette. The calculated concentration of chloroaurate in the toluene was 0.009 M. Gelator **2** (30.0 mg) was suspended in the TOA-Au solution (1.0 mL) and heated to form a solution. The red solution turned colorless before the gel was formed on cooling to RT. The gel was then covered with aqueous lithium borohydride (0.2 M, 0.8 mL). The color of the gel changed to dark purple, which indicated the formation of an AuNPs-containing gel.

Synthesis of platinum nanoparticles: The PtNPs was prepared by using a similar procedure to that described for the AuNPs except 2.5 times the amount of TOAB was used to ensure the uniformity and stability of TOA-Pt in toluene. The color from chloroplatinate was retained until PtNPs were formed on reduction.

- [1] a) B. Escuder, F. Rodriguez-Llansola, J. F. Miravet, *New J. Chem.* **2010**, *34*, 1044–1054; b) N. M. Sangeetha, U. Maitra, *Chem. Soc. Rev.* **2005**, *34*, 821–836; c) X. Y. Liu, *Top. Curr. Chem.* **2005**, *256*, 1–37; d) G. John, S. R. Jadhav, V. M. Menon, V. T. John, *Angew. Chem. Int. Ed.* **2012**, *51*, 1760–1762.
- [2] a) M. George, R. G. Weiss, *Acc. Chem. Res.* **2006**, *39*, 489–497; b) J. H. van Esch, B. L. Feringa, *Angew. Chem.* **2000**, *112*, 2351–2354; *Angew. Chem. Int. Ed.* **2000**, *39*, 2263–2266; c) Y. Gao, F. Zhao, Q. C. Wang, Y. Zhang, *Chem. Soc. Rev.* **2010**, *39*, 3425–3433.
- [3] X. Huang, P. Terech, S. R. Raghavan, R. G. Weiss, *J. Am. Chem. Soc.* **2005**, *127*, 4336–4344.
- [4] a) J. W. Steed, *Chem. Commun.* **2011**, *47*, 1379–1383; b) F. Fages, F. Vögtle, M. Žinič, *Top. Curr. Chem.* **2005**, *256*, 77–131; c) D. J. Abdallah, R. G. Weiss, *J. Braz. Chem. Soc.* **2000**, *11*, 209–218.
- [5] a) S. Nagarajan, P. Ravinder, V. Subramanian, T. M. Das, *New J. Chem.* **2010**, *34*, 123–131; b) T. Tu, W. Assenmacher, H. Peterlik, R. Weisbarth, M. Nieger, K. H. Dötz, *Angew. Chem.* **2007**, *119*, 6486–6490; *Angew. Chem. Int. Ed.* **2007**, *46*, 6368–6371; c) T. Tu, W. Fang, X. Bao, X. Li, K. H. Dötz, *Angew. Chem.* **2011**, *123*, 6731–6735; *Angew. Chem. Int. Ed.* **2011**, *50*, 6601–6605; d) T. Tu, X. Bao, W. Assenmacher, H. Peterlik, J. Daniels, K. H. Dötz, *Chem. Eur. J.* **2009**, *15*, 1853–1861.
- [6] a) M. M. J. Smulders, A. P. H. J. Schenning, E. W. Meijer, *J. Am. Chem. Soc.* **2008**, *130*, 606–611; b) A. R. Hirst, I. A. Coates, T. R. Boucheteau, J. F. Miravet, B. Escuder, V. Castelletto, I. W. Hamley, D. K. Smith, *J. Am. Chem. Soc.* **2008**, *130*, 9113–9121.
- [7] a) Y.-B. He, Z. Bian, C.-Q. Kang, L.-X. Gao, *Chem. Commun.* **2011**, *47*, 1589–1591; b) Y.-B. He, Z. Bian, C.-Q. Kang, L.-X. Gao, *Chem. Commun.* **2010**, *46*, 5695–5697.
- [8] a) Y.-J. Wang, L.-M. Tang, J. Yu, *Cryst. Growth Des.* **2008**, *8*, 884–889; b) O. Lebel, M.-È. Perron, T. Maris, S. F. Zalzal, A. Nanci, J. D. Wuest, *Chem. Mater.* **2006**, *18*, 3616–3626; c) D. K. Kumar, D. A. Jose, A. Das, P. Dastidar, *Chem. Commun.* **2005**, 4059–4061; d) P. Terech, N. M. Sangeetha, U. Maitra, *J. Phys. Chem. B* **2006**, *110*, 15224–15233.
- [9] a) U. Gasser, B. Sierra-Martín, A. Fernandez-Nieves, *Phys. Rev. E* **2009**, *79*, 051403; b) F. Andrea, S. Eduardo, D. Marjolein, *Phys. Rev. E* **2008**, *78*, 041402; c) N. M. Dixit, C. F. Zukoski, *Phys. Rev. E* **2003**, *67*, 061501.
- [10] a) J. Gan, M. E. Bakkari, C. Belin, C. Margottin, P. Godard, J.-L. Pozzo, J.-M. Vincent, *Chem. Commun.* **2009**, 5133–5134; b) A. Raghavanpillai, S. Reinartz, K. W. Hutchenson, *J. Fluorine Chem.* **2009**, *130*, 410–417; c) J. Loiseau, M. Lescanne, A. Colin, F. Fages, J.-B. Verlhac, J.-M. Vincent, *Tetrahedron* **2002**, *58*, 4049–4052; d) E. Faggi, R. M. Sebastián, A. Vallribera, *Tetrahedron* **2010**, *66*, 5190–5195; e) M. Yamanaka, Y. Miyake, S. Akita, K. Nakano, *Chem. Mater.* **2008**, *20*, 2072–2074.
- [11] M. George, S. L. Snyder, P. Terech, C. J. Glinka, R. G. Weiss, *J. Am. Chem. Soc.* **2003**, *125*, 10275–10283.
- [12] a) A. R. Borges, M. Hyacinth, M. Lum, C. M. Dingle, P. L. Hamilton, M. Chruszcz, L. Pu, M. Sabat, K. L. Caran, *Langmuir* **2008**, *24*, 7421–7431.
- [13] a) T. S. Thakur, M. T. Kirchner, D. Bläser, R. Boese, G. R. Desiraju, *CrystEngComm* **2010**, *12*, 2079–2085; b) H. Y. Lee, A. Olasz, M. Pink, H. Park, D. Lee, *Chem. Commun.* **2011**, *47*, 481–483; c) M. Horiguchi, S. Okuhara, E. Shimano, D. Fujimoto, H. Takahashi, H. Tsue, R. Tamura, *Cryst. Growth Des.* **2008**, *8*, 540–548; d) J.-L. Syssa-Magalé, K. Boubekeur, P. Palvadeau, A. Meerschaert, B. Schöllhorn, *CrystEngComm* **2005**, *7*, 302–308; e) F. Fontana, A. Forni, P. Metrangolo, W. Panzeri, T. Pilati, G. Resnati, *Supramol. Chem.* **2002**, *14*, 47–55.
- [14] a) K. J. C. van Bommel, A. Friggeri, S. Shinkai, *Angew. Chem.* **2003**, *115*, 1010–1030; *Angew. Chem. Int. Ed.* **2003**, *42*, 980–999; b) D. Das, T. Kar, P. K. Das, *Soft Matter* **2012**, *8*, 2348–2365.
- [15] a) P. K. Vemula, G. John, *Chem. Commun.* **2006**, 2218–2220; b) S. Ray, A. K. Das, A. Banerjee, *Chem. Commun.* **2006**, 2816–2818; c) N. M. Sangeetha, S. Bhat, G. Raffy, C. Belin, A. Loppinet-Serani, C. Aymonier, P. Terech, U. Maitra, J. P. Desvergne, A. Del Guerso, *Chem. Mater.* **2009**, *21*, 3424–3432; d) X. Wang, C. E. Egan, M. Zhou, K. Prince, D. R. G. Mitchell, R. A. Caruso, *Chem. Commun.* **2007**, 3060–3062; e) J. H. Lee, S. Kang, J. Y. Lee, J. H. Jung, *Soft Matter* **2012**, *8*, 2557–2563; f) M.-O. M. Piepenbrock, N. Clarke, J. W. Steed, *Soft Matter* **2011**, *7*, 2412–2418; g) T. Kar, S. Dutta, P. K. Das, *Soft Matter* **2010**, *6*, 4777–4787; h) L.-S. Li, S. I. Stupp, *Angew. Chem.* **2005**, *117*, 1867–1870; *Angew. Chem. Int. Ed.* **2005**, *44*, 1833–1836.
- [16] I. Maity, D. B. Rasale, A. K. Das, *Soft Matter* **2012**, *8*, 5301–5308.
- [17] a) M. S. Lamm, N. Sharma, K. Rajagopal, F. L. Beyer, J. P. Schneider, D. J. Pochan, *Adv. Mater.* **2008**, *20*, 447–451; b) J.-L. Li, X.-Y. Liu, X.-G. Wang, R.-Y. Wang, *Langmuir* **2011**, *27*, 7820–7827.
- [18] C.-Q. Kang, Z. Bian, Y.-B. He, F.-S. Han, X.-P. Qiu, L.-X. Gao, *Chem. Commun.* **2011**, *47*, 10746–10748.
- [19] S. Aubry, S. Pellet-Rostaing, R. Faure, M. Lemaire, *J. Heterocycl. Chem.* **2006**, *43*, 139–148.
- [20] C. Kang, Z. Du, L. Wang, Y. Chen, X. Qiu, H. Guo, L. Gao, *Chem. Res. Chin. Univ.* **2012**, *28*, 843–848.
- [21] W. Edwards, C. A. Lagadec, D. K. Smith, *Soft Matter* **2011**, *7*, 110–117.
- [22] L. M. Salonen, M. Ellermann, F. Diederich, *Angew. Chem.* **2011**, *123*, 4908–4944; *Angew. Chem. Int. Ed.* **2011**, *50*, 4808–4842.
- [23] a) I. Kapoor, E.-M. Schön, J. Bachl, D. Kühbeck, C. Catiavela, S. Saha, R. Banerjee, S. Roelens, J. J. Marrero-Tellado, D. D. Diaz, *Soft Matter* **2012**, *8*, 3446–3456; b) D. J. Adams, K. Morris, L. Chen, L. C. Serpell, J. Bacsá, G. M. Day, *Soft Matter* **2010**, *6*, 4144–4156.
- [24] a) J. U. Kim, D. Schollmeyer, M. Brehmer, R. Zentel, *J. Colloid Interface Sci.* **2011**, *357*, 428–433; b) V. Čaplar, L. Frkanec, N. S. Vujčić, M. Žinič, *Chem. Eur. J.* **2010**, *16*, 3066–3082; c) V. Čaplar, M. Žinič, J.-L. Pozzo, F. Fages, G. Mieden-Gundert, F. Vögtle, *Eur. J. Org. Chem.* **2004**, 4048–4059; d) Y. Watanabe, T. Miyasou, M. Hayashi, *Org. Lett.* **2004**, *6*, 1547–1550.
- [25] C. S. Love, V. Chechik, D. K. Smith, K. Wilson, I. Ashworth, C. Brennan, *Chem. Commun.* **2005**, 1971–1973.
- [26] B. Li, D. C. Higgins, S. Zhu, H. Li, H. Wang, J. Ma, Z. Chen, *Catal. Commun.* **2012**, *18*, 51–54.
- [27] Y. Song, R. M. Garcia, R. M. Dorin, H. Wang, Y. Qiu, E. N. Coker, W. A. Steen, J. E. Miller, J. A. Shelnut, *Nano Lett.* **2007**, *7*, 3650–3655.
- [28] M. Kimura, S. Kobayashi, T. Kuroda, K. Hanabusa, H. Shirai, *Adv. Mater.* **2004**, *16*, 335–338.
- [29] a) E. G. Bilé, E. Cortelazzo-Polisini, A. Denicourt-Nowicki, R. Sassine, F. Launay, A. Roucoux, *ChemSusChem* **2012**, *5*, 91–101; b) N. Asim, S. Radiman, M. A. Yarmo, M. S. B. Golriz, *Microporous Mesoporous Mater.* **2009**, *120*, 397–401; c) O. R. Miranda, N. R. Dollahon, T. S. Ahmadi, *Cryst. Growth Des.* **2006**, *6*, 2747–2753; d) E. G. Bilé, R. Sassine, A. Denicourt-Nowicki, F. Launay, A. Roucoux, *Dalton Trans.* **2011**, *40*, 6524–6531.
- [30] G. M. Sheldrick, *Acta Crystallogr. A* **2008**, *64*, 112–122.

Received: July 24, 2012
Published online: November 4, 2012